

Chemical Sciences Division. R.H. acknowledges support by the donors of the Petroleum Research Fund, administered by the American Chemical Society, and support from the National Institutes of General Medical Sciences (GM33828). We also thank Pat Cyr for experimental assistance.

**Supplementary Material Available:** Tables of positional and anisotropic thermal parameters, bond lengths, and bond angles (14 pages); tables of calculated and observed structure factors (7 pages). Ordering information is given on any current masthead page.

## Effects of Solvents, Axial Ligation, and Radical Cation Formation on the V=O Stretching Raman Frequency in Vanadyl Porphyrins: Implications for Peroxidase Intermediates

Y. Oliver Su,<sup>†</sup> Roman S. Czernuszewicz, Lisa A. Miller, and Thomas G. Spiro\*

Contribution from the Department of Chemistry, Princeton University, Princeton, New Jersey 08544. Received August 27, 1987

**Abstract:** The systematics of the V=O stretching frequency in vanadyl porphyrins are investigated with resonance Raman (RR) spectroscopy. For a series of solvents the frequency decreases with increasing solvent acceptor number, consistent with solvent-induced polarization of the V-O bond. Variations in the solvent dependence are seen for different porphyrins, reflecting different polarization effects of the peripheral substituents. In coordinating solvents a second V-O stretching band, at lower frequency, arises from six-coordinate species. The downshift in  $\nu_{V-O}$  upon ligation increases with increasing donor strength of the ligand. It is larger for imidazolate than imidazole, and it is especially large for hydroxide; the hydroxide effect is attributed to  $OH^- \rightarrow V^{IV} \pi$ -donation, competing with the oxo ligand for acceptor d orbitals. The RR spectrum of (VO)OEP<sup>•+</sup> produced by electrochemical oxidation shows porphyrin skeletal mode frequency shifts similar to those seen for other OEP  $\pi$ -cation radicals. The V-O stretching frequency increases 15  $cm^{-1}$  relative to (VO)OEP. These findings are discussed in relation to recent RR data on ferryl porphyrins and ferryl species in heme proteins. Differences among these species can be accounted for on the basis of proximal and distal effects.

Oxometal complexes are implicated in oxygen activation by heme proteins. The peroxidase intermediates, compounds I and II, are known to contain ferryl heme.<sup>1-3</sup> This species is also believed to participate in the mechanism of catalytic oxidation and hydroxylation by cytochrome P<sub>450</sub> enzymes.<sup>4,5</sup> Considerable progress has been made in probing the nature of the Fe-O bond via EXAFS<sup>6-9</sup> and resonance Raman (RR) spectroscopies.<sup>10-18</sup> RR studies of horseradish peroxidase (HRP) compound II<sup>10,13,16,17</sup> and the ES complex of cytochrome c peroxidase (CCP)<sup>14,18</sup> reveal a bond of moderate strength. In HRP the O atom is H-bonded to a titratable distal residue, probably histidine. In order to evaluate the resonance Raman evidence it is desirable to examine reference complexes with systematic variation of both distal and proximal interactions. In addition, since compound I of peroxidases contains a ferryl porphyrin  $\pi$ -cation radical, it is of interest to anticipate the effect on the Fe=O bond of ring oxidation.

Isolated ferryl porphyrins have yielded informative RR spectra<sup>19-22</sup> but are of limited stability and do not readily lend themselves to systematic studies. Accordingly we have turned to vanadyl porphyrin, which has a stable V-O bond,<sup>23</sup> and can be examined in a variety of environments. In this study we evaluate solvent effects, including H-bonding, axial ligand interactions, and radical cation formation on the stretching frequency of the V-O bond, as monitored by RR spectroscopy. These frequency variations throw light on the available data for ferryl hemes and allow evaluation of the chemical interactions in the binding pocket of ferryl heme-containing proteins.

### Experimental Section

Vanadyl complexes of octaethylporphyrin (OEP), tetraphenylporphyrin (TPP), and tetrakis(methylpyridinium)porphyrin (TMPyP) were purchased from Mid Centry Chemicals (Posen, IL). They were

dissolved in spectral grade solvents, and their UV-vis spectra were checked. When necessary they were chromatographed on alumina (A

- (1) Critchlow, J. E.; Dunford, H. B. *J. Biol. Chem.* **1972**, *247*, 3714-3725.
- (2) Roberts, J. E.; Hoffman, B. H.; Rutter, R.; Hager, L. P. *J. Am. Chem. Soc.* **1981**, *103*, 7654-7656.
- (3) LaMar, G. N.; DeRopp, J. S.; Latos-Grazynsky, L.; Balch, A. L.; Johnson, R. B.; Smith, K. M.; Parish, D. W.; Chen, R. *J. Am. Chem. Soc.* **1983**, *105*, 782-787.
- (4) Griffin, B. W.; Peterson, J. A.; Estabrook, R. W. In *Porphyrins*; Dolphin, D., Ed.; Academic: New York, 1979; Vol. 7, p 333.
- (5) White, R. E.; Coon, M. J. *Annu. Rev. Biochem.* **1980**, *49*, 315-356.
- (6) Penner-Hahn, J. E.; McMurry, T. J.; Renner, M.; Latos-Grazynsky, L.; Eble, A. S.; Davis, I. M.; Balch, A. L.; Groves, J. T.; Dawson, J. H.; Hodgson, K. O. *J. Biol. Chem.* **1983**, *258*, 12761-12764.
- (7) Penner-Hahn, J. E.; Eble, K. S.; McMurry, T. J.; Renner, M.; Balch, A. L.; Groves, J. T.; Dawson, J. H.; Hodgson, K. O. *J. Am. Chem. Soc.* **1986**, *108*, 7819-7825.
- (8) Chance, M.; Powers, L.; Kumar, C.; Chance, B. *Biochemistry* **1986**, *25*, 1259-1265.
- (9) Chance, M.; Powers, L.; Poulos, T.; Chance, B. *Biochemistry* **1986**, *25*, 1266-1270.
- (10) Termer, J.; Sitter, A. J.; Reczek, C. M. *Biochim. Biophys. Acta* **1985**, *828*, 73-80.
- (11) Sitter, A. J.; Reczek, C. M.; Termer, J. *Biochim. Biophys. Acta* **1985**, *828*, 229-235.
- (12) Sitter, A. J.; Reczek, C. M.; Termer, J. *J. Biol. Chem.* **1985**, *260*, 7515-7520.
- (13) Sitter, A. J.; Reczek, C. M.; Termer, J. *J. Biol. Chem.* **1986**, *261*, 8638-8642.
- (14) Sitter, A. J.; Reczek, C. M.; Termer, J., manuscript in preparation.
- (15) Hashimoto, S.; Tatsuno, Y.; Kitagawa, T. *Proc. Jpn. Acad. Ser. B. Phys. Biol. Sci.* **1984**, *60*, 345-348.
- (16) Hashimoto, S.; Tatsuno, Y.; Kitagawa, T. *Proc. Natl. Acad. Sci. U.S.A.* **1986**, *83*, 2417-2421.
- (17) Hashimoto, S.; Teraoka, J.; Inubushi, T.; Yonetani, T.; Kitagawa, T. *J. Biol. Chem.* **1986**, *261*, 11110-11118.
- (18) Makino, R.; Uno, T.; Nishimura, Y.; Iizuka, T.; Tsuboi, M.; Ishimura, Y. *J. Biol. Chem.* **1986**, *261*, 8376-8382.
- (19) (a) Bajdor, K.; Nakamoto, K. *J. Am. Chem. Soc.* **1984**, *106*, 3045.
- (b) Proniewicz, J. M.; Bajdor, K.; Nakamoto, K. *J. Phys. Chem.* **1986**, *90*, 1760-1766.

\* Author to whom correspondence should be addressed.

<sup>†</sup> Present address: Department of Chemistry, National Taiwan University, Taipei, Taiwan, Republic of China.

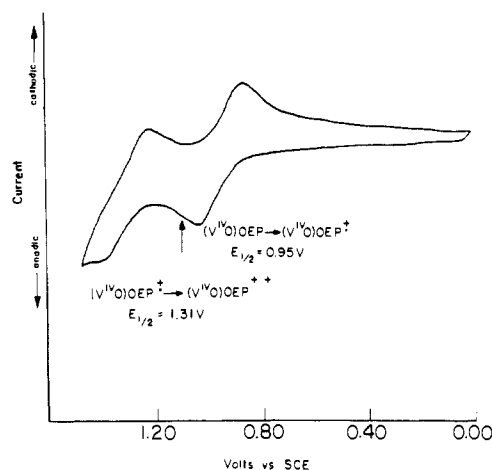


**Figure 1.** Cyclic voltammogram of (VO)OEP (0.5 mM) in  $\text{CH}_2\text{Cl}_2$  containing 0.1 M tetrabutylammonium perchlorate, showing oxidation processes involving porphyrin  $\pi$ -cation radical formation. The arrow marks the potential used for electrolytic generation of (VO)OEP $^{2+}$  for RR studies.

540) to remove fluorescing impurities. To prepare  $^{18}\text{O}$ -labeled (VO)OEP, a fivefold excess of  $\text{VCl}_3$  was added to OEP free base in dried, distilled, and degassed (freeze-pump-thaw) dimethylformamide, and the solution was refluxed under an  $^{18}\text{O}_2$  atmosphere for 2 h. The product was precipitated with cold water, washed to remove excess  $\text{VCl}_3$ , dissolved in methylene chloride, and chromatographed on alumina to remove unreacted free-base porphyrin. Raman spectroscopy showed the resulting (VO)OEP to contain a 60/40 mixture of  $^{18}\text{O}$  and  $^{16}\text{O}$ .

Raman spectra were obtained via backscattering from spinning NMR tubes, with a SPEX 1401 double monochromator equipped with a cooled RCA 31034A photomultiplier and photon counting electronics (ORTEC 9315), with laser excitation at 406.7 (Spectra Physics 171 Kr $^+$ ) or 441.6 nm (LiCONIX 4042PS He-Cd). The data were collected digitally with a MINC II (DEC) computer. Relatively low laser power levels (10 mW) were used in order to avoid photodegradation of the samples. Spectra were recorded with a 5  $\text{cm}^{-1}$  slit width, a 1 s time constant, and a 1.0  $\text{cm}^{-1}/\text{s}$  scan rate.

Cyclic voltammetry and controlled potential electrolysis of (VO)OEP were carried out in  $\text{CH}_2\text{Cl}_2$  with tetrabutylammonium perchlorate as supporting electrolyte, using a PAR 173 potentiostat, 175 programmer, and 179 coulometer. A three-electrode bulk electrolysis Raman cell, $^{29c}$  with Pt gauze working electrode, saturated calomel (SCE) reference electrode, and Pt wire auxiliary electrode, was used for oxidation of (VO)OEP and subsequent Raman measurements. The design of the cell allowed for Raman spectra to be recorded in situ in backscattering geometry.

## Results

**(VO)OEP $^{2+}$   $\pi$ -Cation Radical.** Figure 1 shows the oxidation cyclic voltammogram of (VO)OEP in  $\text{CH}_2\text{Cl}_2$ . Redox waves for porphyrin mono- and dication formation are well formed. The (VO)OEP $^{2+}$  reduction potential, +0.95 V versus SCE, is  $\sim 0.2$  V lower than for (VO)TPP $^{2+}$ , $^{24}$  as expected from other OEP/TPP comparisons. $^{25}$  The arrow marks the potential, +1.10 V versus SCE, applied for coulometric generation of (VO)OEP $^{2+}$ .

Figure 2 shows RR spectra for the neutral (VO)OEP porphyrin and  $\pi$ -cation radical of samples containing  $^{16}\text{O}$  and  $^{18}\text{O}$ , using 406.7-nm excitation. The V=O stretching bands, $^{23b}$  at 987  $\text{cm}^{-1}$  for (VO)OEP and 1002  $\text{cm}^{-1}$  for (VO)OEP $^{2+}$ , are readily identified by their 42–43  $\text{cm}^{-1}$   $^{18}\text{O}$  shifts; for a diatomic V=O oscillator,

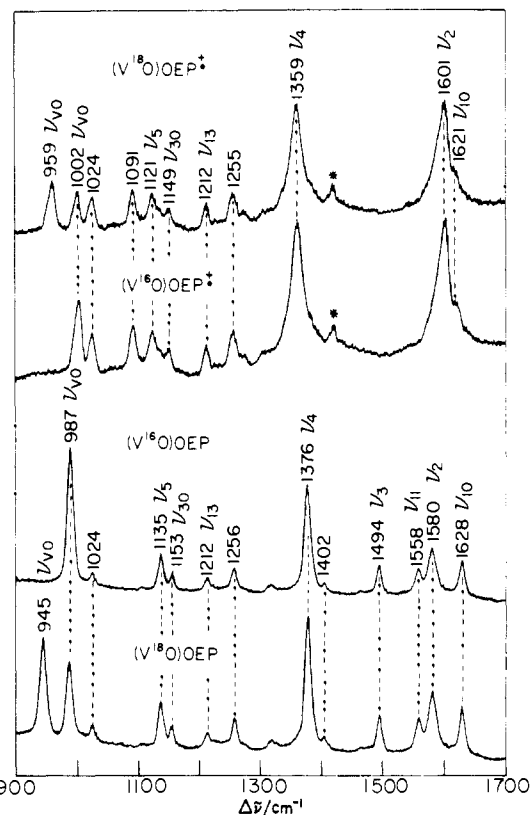


**Figure 2.** RR spectra with excitation at 406.7 nm, near resonance with the Soret bands of (VO)OEP (406 nm) and (VO)OEP $^{2+}$  (397 nm). The V=O stretching bands, at 987 and 1002  $\text{cm}^{-1}$ , shift down on  $^{18}\text{O}$  substitution to 945 and 959  $\text{cm}^{-1}$ , respectively. Residual bands at the  $^{16}\text{O}$  positions are due to incomplete isotope incorporation. The asterisk indicates a 1423  $\text{cm}^{-1}$   $\text{CH}_2\text{Cl}_2$  solvent band.

**Table I.** Five-Coordinate Vanadyl Porphyrin V=O Stretching Frequencies ( $\text{cm}^{-1}$ )

solvent	acceptor no.	OEP	TPP	TMPyP
hexane	0	1007	1007	
THF	8.0	998		
benzene	8.2	997	1001	
piperidine	?	1000	1003	
pyridine	14.2	992	997	
nitrobenzene	14.8	990		
DMF	16.0	991	998	
$\text{CH}_3\text{CN}$	19.3	988	996	1005
$\text{CH}_2\text{Cl}_2$	20.4	987	995	
$\text{CH}_3\text{NO}_2$	20.5	987		1004
$\text{CHCl}_3$	23.1	984	992	
2-propanol	33.5	985	991	1010
ethanol	37.1	983	989	987
methanol	41.3	980	987	984
water	54.8			970

a 43- $\text{cm}^{-1}$  shift is expected. The V=O stretch shifts up 15  $\text{cm}^{-1}$  upon ring oxidation, implying a strengthening of the V=O bond. The residual peaks at the  $\text{V}^{16}\text{O}$  positions in the  $\text{V}^{18}\text{O}$  spectra are due to incomplete isotope incorporation (see Experimental Section).

The remaining RR bands arise from porphyrin skeletal modes, $^{26}$  as indicated in Figure 2. Because the excitation, 406.7 nm, is near resonance with the strong Soret bands (406 nm for (VO)OEP, 397 nm for (VO)OEP $^{2+}$ ), the RR spectra show strong enhancement for totally symmetric ( $A_1$ ) modes, particularly,  $\nu_2$  and  $\nu_4$ . $^{27}$  Several non-totally symmetric modes are also prominent, however, particularly  $\nu_{10}$  and  $\nu_{11}$  ( $B_1$  modes), probably due to Jahn-Teller

(20) Hashimoto, S.; Tatsuno, Y.; Kitagawa, T. In *Proceedings of the Tenth International Conference on Raman Spectroscopy*; Peticolas, W. L., Hudson, B., Eds.; University of Oregon, Eugene, Oregon, 1986; pp 1–29.

(21) Schappacher, M.; Chottard, G.; Weiss, R. *J. Chem. Soc., Chem. Commun.* **1986**, 93–94.

(22) Kean, R. T.; Oertling, W. A.; Babcock, G. T. *J. Am. Chem. Soc.* **1987**, *109*, 2185–2187.

(23) (a) Pettersen, R. C.; Alexander, L. E. *J. Am. Chem. Soc.* **1968**, *90*, 3873–3875. (b) Buchler, J. W.; Puppe, L.; Rohbock, K.; Schneehage, H. H. In *Ann. N.Y. Acad. Sci.* **1973**, *206*, 116.

(24) Kadish, K. M.; Morrison, M. M. *Bioinorg. Chem.* **1977**, *7*, 107–115.

(25) Kadish, K. M. In *Iron Porphyrins*; Lever, A. B. P., Gray, H. B., Eds.; Addison-Wesley: Reading, MA, 1983; Part 11, pp 161–250.

(26) Abe, M.; Kitagawa, T.; Kyogoku, Y. *J. Chem. Phys.* **1978**, *69*, 4526–4534.

(27) Spiro, T. G. In *Iron Porphyrins*; Lever, A. B. P., Gray, H. B., Eds.; Addison-Wesley: Reading, MA, 1983; Part 11, pp 89–159.

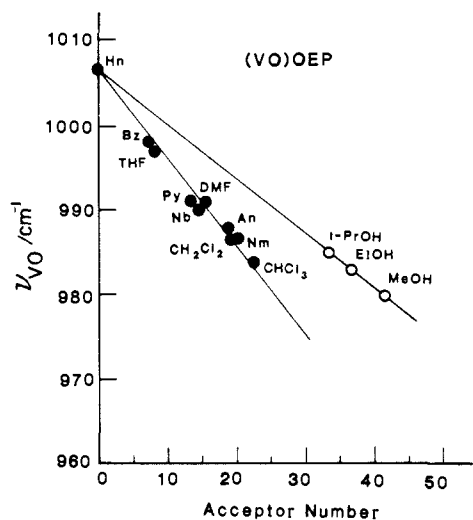


**Figure 3.** Plot of (VO)OEP V-O stretching frequency as a function of the solvent acceptor number. Symbols: Hn, hexane; Bz, benzene; THF, tetrahydrofuran; Py, pyridine; DMF, dimethylformamide; Nb, nitrobenzene; An, acetonitrile; Nm, nitromethane; i-PrOH, isopropyl alcohol, (2-propanol); EtOH, ethanol; MeOH, methanol.

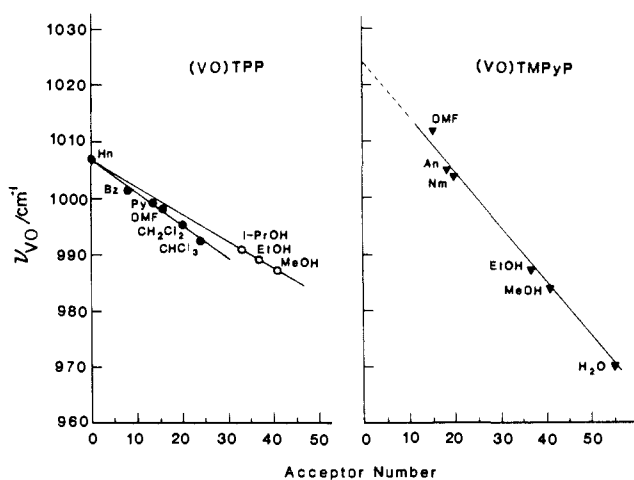


**Figure 4.** As Figure 3, but for (VO)TPP and (VO)TMPyP.

splitting of the excited state.<sup>28</sup> The (VO)OEP<sup>++</sup> bands are readily correlated with those of (VO)OEP on the basis of the intensity pattern. Most frequency shifts are small, but  $\nu_2$  and  $\nu_4$  show large up- and downshifts, +21 and -17  $\text{cm}^{-1}$ , respectively, upon radical cation formation. This shift pattern is consistent<sup>29</sup> with those seen for NiOEP and CuOEP  $\pi$ -cation radicals.<sup>30</sup>

**Solvent Effects on the V-O Stretching Frequency.** The V-O stretching RR band was monitored in a series of solvents for (VO)OEP, (VO)TPP, and (VO)TMPyP. The frequencies are listed in Table II and plotted in Figures 3 and 4 against the solvent acceptor number (AN), as determined by Gutman and co-workers.<sup>31</sup> In all cases the V-O frequency decreases with increasing AN, implying that stronger acceptor solvents weaken the V-O bond. Straight lines are obtained, although the alcohol

**Table II.** Six- versus Five-Coordinate V-O Stretching Frequencies ( $\text{cm}^{-1}$ )

ligand	solvent	porphyrin	5-c <sup>a</sup>	6-c <sup>a</sup>	$\Delta(5-6)^a$
H <sub>2</sub> O	water	TMPyP	970	955	15
CH <sub>3</sub> OH	methanol	TMPyP	984	969	15
CH <sub>3</sub> OH	methanol	TPP	987	965	22
CH <sub>3</sub> OH	methanol	OEP	980	965	15
C <sub>2</sub> H <sub>5</sub> OH	ethanol	TMPyP	987	974	13
Py	pyridine	TPP	997	975	22
Py	pyridine	OEP	992	973	19
Pip	piperidine	TPP	1003	985	18
Pip	piperidine	OEP	1000	985	15
THF	THF	OEP	998	990	8
ImH	CH <sub>3</sub> CN	TMPyP	1006	960	46
ImH	CH <sub>3</sub> CN	TPP	996	959	37
ImH	CH <sub>3</sub> CN	OEP	988	955	33
Im <sup>-</sup>	CH <sub>3</sub> CN	TPP	996	936	60
Im <sup>-</sup>	CH <sub>3</sub> CN	OEP	988	933	55
OH <sup>-</sup>	water	TMPyP	970	895	75

<sup>a</sup> 5-c, five-coordinate (VO) porphyrin; 6-c, six-coordinate adduct with the indicated ligand;  $\Delta(5-6)$ , frequency difference between 5-c and 6-c.

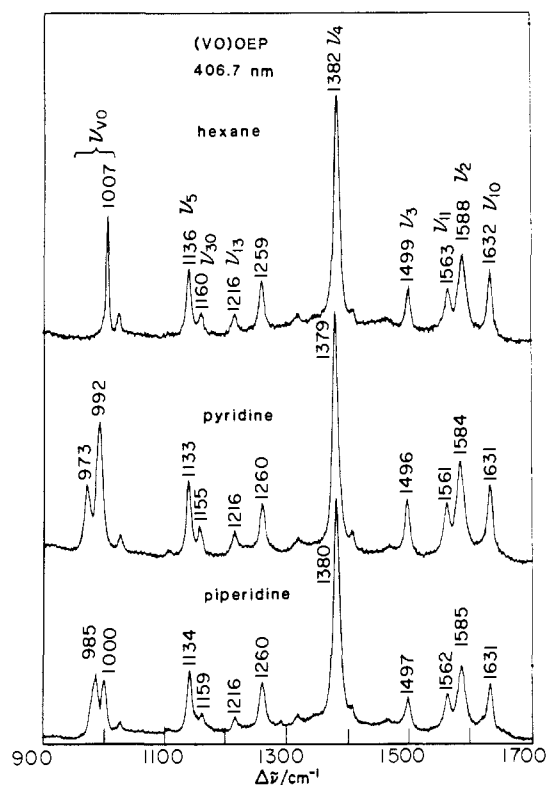


**Figure 5.** RR spectra with 406.7-nm excitation of (VO)OEP in hexane, pyridine, and piperidine. The bands at 973 and 985  $\text{cm}^{-1}$  in the latter two spectra are attributed to six-coordinate species in the ligating solvents.

solvents fall on a separate line from the remaining solvents for (VO)OEP and (VO)TPP, but not for (VO)TMPyP. The slopes differ markedly for OEP and TPP. They are 0.65 (alcohols) and 1.0 (other solvents)  $\text{cm}^{-1}/\text{AN}$  for OEP, but 0.46 and 0.54  $\text{cm}^{-1}/\text{AN}$  for TPP. The intercepts, however, are all the same, 1006  $\text{cm}^{-1}$ , which is the actual value measured in hexane (AN = 0) for both (VO)OEP and VO(TPP). The intercept is significantly higher, 1024  $\text{cm}^{-1}$ , for (VO)TMPyP (which is insoluble in hexane), while the slope, 0.96  $\text{cm}^{-1}/\text{AN}$ , is as high as the higher of the OEP slopes. Thus, the three porphyrins show differences with respect to the V-O bond strength and its susceptibility to solvent-induced weakening.

**Six-Coordinate Species.** Figure 5 shows RR spectra for (VO)OEP in hexane, pyridine, and piperidine. The single strong V-O stretching band at 1007  $\text{cm}^{-1}$  in hexane is replaced by a pair of bands in pyridine (992, 973  $\text{cm}^{-1}$ ) and piperidine (1000, 985

(28) Cheung, D.; Yu, N.-T.; Felton, R. H. *Chem. Phys. Lett.* **1978**, *55*, 527-530.

(29) (a) Kim, D.; Miller, L. A.; Rakhit, G.; Spiro, T. G. *J. Phys. Chem.* **1986**, *90*, 3320-3325. We note that the  $a_{1g}$  radical cation data in this reference are incorrect due to interference from porphyrin diacid signals as noted by Oertling et al.<sup>29b</sup> (b) Oertling, W. A.; Salchi, A.; Chang, C. K.; Babcock, G. T. *J. Phys. Chem.* **1987**, *91*, 3114-3116. (c) Czernuszewicz, R. S.; Macor, K. A.; Li, X.-Y.; Kincaid, J. R.; Spiro, T. G., manuscript in preparation.

(30) Fajer, J.; Davis, M. S. In *The Porphyrins*; Dolphin, D., Ed.; Academic: New York, 1978; Vol. IV; pp 197-256.

(31) (a) Mayer, U.; Gutmann, V.; Gerger, W. *Monatsh. Chem.* **1975**, *106*, 1235-1257. (b) Gutmann, V. *Electrochem. Acta* **1976**, *21*, 661-670. (c) Gutmann, V. *The Donor-Acceptor Approach to Molecular Interactions*; Plenum: New York, 1978.

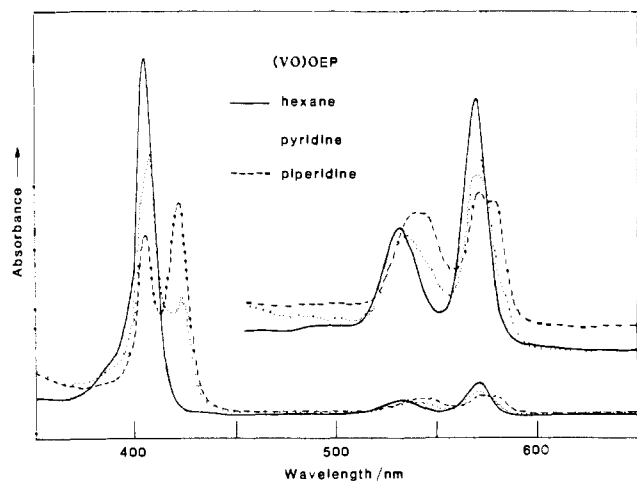


Figure 6. Optical absorption spectra for (VO)OEP in hexane, pyridine, and piperidine. The split peaks in the latter two solvents reflect the 5-/6-coordinate equilibrium.

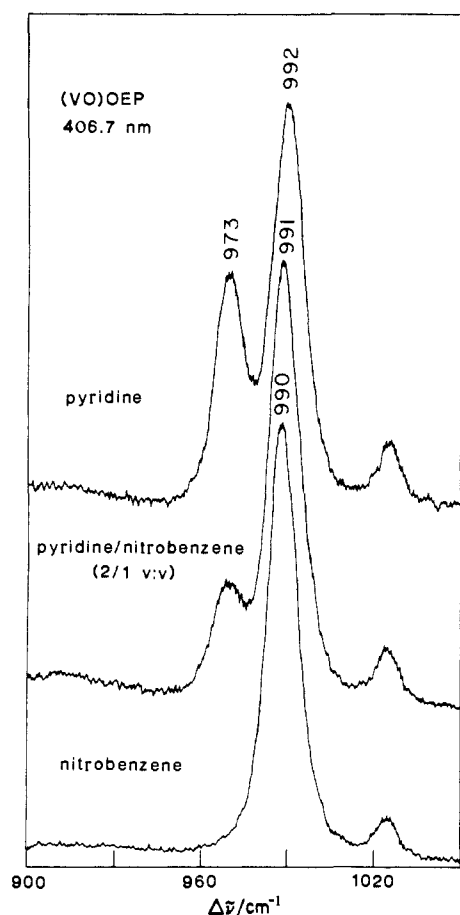


Figure 7. The V-O stretching region of the 406.7-nm-excited RR spectra for (VO)OEP in nitrobenzene, pyridine, and a 2:1 pyridine:nitrobenzene mixture, showing the 6-coordinate 973  $\text{cm}^{-1}$  band growing in with increasing pyridine concentration.

$\text{cm}^{-1}$ ). We attribute the lower of these two bands to a six-coordinate species, produced by axial ligation of the coordinating solvents. The larger intensity ratio in piperidine relative to pyridine for the 6- versus 5-coordinate bands is consistent with piperidine, a stronger base, binding more strongly than pyridine. Small differences, up to 3  $\text{cm}^{-1}$ , were seen among the three spectra for the porphyrin skeletal modes,  $\nu_2$ ,  $\nu_3$ , and  $\nu_4$ ,<sup>26</sup> which are known to be susceptible to a variety of electronic influences at the central metal ion.<sup>27</sup> Figure 6 shows absorption spectra for (VO)OEP in the same solvents. The doubled bands seen for pyridine and piperidine are likewise indicative of 6-/5-coordinate mixtures. The

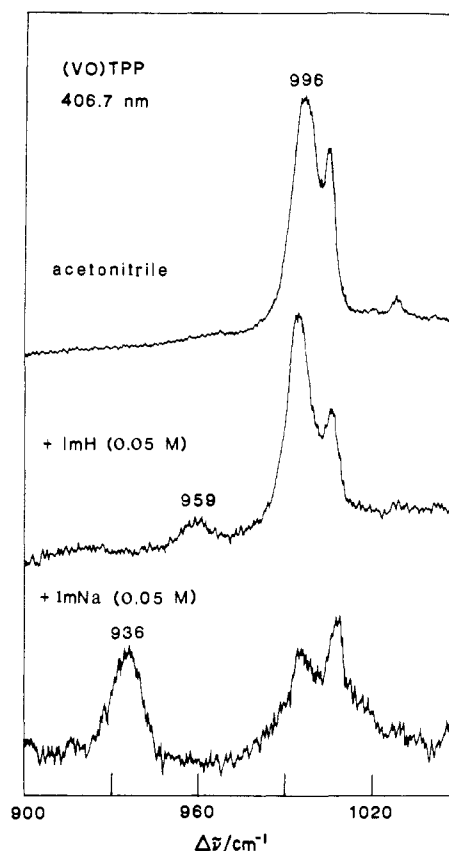


Figure 8. The V-O stretching region of the 406.7-nm-excited RR spectra of (VO)TPP (0.1 mM) in acetonitrile and with added imidazole (0.05 M) and sodium imidazolate (0.05 M) solubilized with the 15-crown-5 crown ether, showing the downshifted 6-coordinate peaks at 959 and 936  $\text{cm}^{-1}$ .

comparable 6- and 5-coordinate populations in the pure donor solvents show that adduct formation is relatively weak. The weakness of the binding is no doubt a reflection of strong electron donation from the oxo ligand (see Discussion section), which lowers the effective charge on the  $\text{V}^{\text{IV}}$  center substantially. The out-of-plane displacement, 0.5 Å,<sup>23a</sup> of the V atom in the five-coordinate VO porphyrin is also a contributing factor.

Proof that it is the lower of the two V-O RR bands that arise from 6-coordinate adduct is shown in Figure 7. As pyridine is added to (VO)OEP in nitrobenzene (whose 5-coordinate V-O band is at the same frequency as in pyridine) the lower frequency band at 973  $\text{cm}^{-1}$  grows in proportion to the amount of pyridine. Stronger ligands produce 6-coordinate bands at lower concentrations. Figure 8 shows that adding ~0.05 M imidazole (ImH) to (VO)TPP in acetonitrile produces a new band at 959  $\text{cm}^{-1}$ , while adding the same concentration of sodium imidazolate, solubilized with the crown ether 15-crown-5, produces a stronger band at 936  $\text{cm}^{-1}$ , together with a weakening of the 996- $\text{cm}^{-1}$  5-coordinate band.

Figure 9 shows RR spectra in the (VO) stretching region for (VO)TMPyP in  $\text{H}_2\text{O}$  or  $\text{D}_2\text{O}$  at neutral and alkaline pH (pD). At high pH the strong 955- $\text{cm}^{-1}$  band is replaced by one at 895  $\text{cm}^{-1}$ . Assignment of both bands to V-O stretching was confirmed by their shifts, to 916 and 858  $\text{cm}^{-1}$ , when the solutions were made up in  $\text{H}_2^{18}\text{O}$ . Interestingly the  $^{18}\text{O}/^{16}\text{O}$  exchange process was quite slow at pH 7, taking ~3 h of equilibration, but was complete within the measurement time (~10 min) at pH 13. Thus the exchange relation is base catalyzed (see Discussion).

When (VO)TMPyP is dissolved in methanol, the RR spectrum (not shown) displays a strong band at 984  $\text{cm}^{-1}$  and a weaker one, attributed to the 6-coordinate adduct, at 969  $\text{cm}^{-1}$ . As water is mixed with the methanol, both bands shift down, and the lower frequency band intensifies at the expense of the higher frequency band, which disappears in pure water. The frequency of the upper

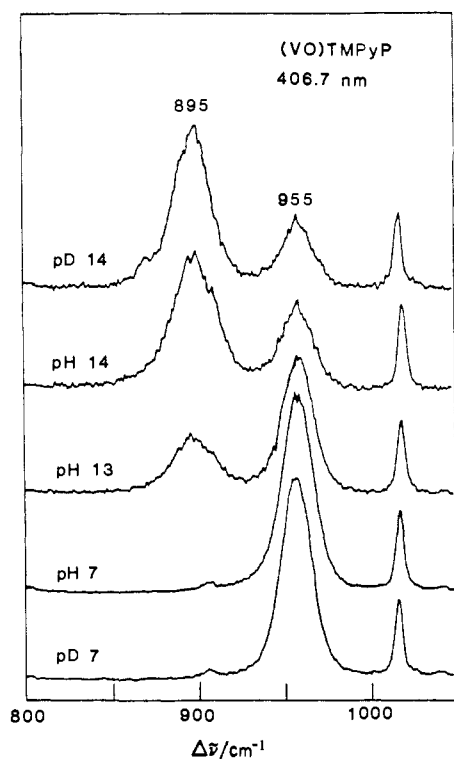


**Figure 9.** The V–O stretching region of the 406.7-nm-excited RR spectra for (VO)TMPyP in water and D<sub>2</sub>O at various pH (pD) values. The 955 and 895 cm<sup>-1</sup> bands are attributed to 6-coordinate species with H<sub>2</sub>O and OH<sup>-</sup> ligands.

band when extrapolated to pure water is 970 cm<sup>-1</sup>; this is the value expected for water from the linear plot of 5-coordinate V–O frequency versus solvent acceptor number, as shown in Figure 3. Thus the strong 955-cm<sup>-1</sup> band in water is assigned to the 6-coordinate aquo adduct of (VO)TMPyP. The 15-cm<sup>-1</sup> downshift from the 5-coordinate frequency is the same as that shown by the methanol adduct.

The 895-cm<sup>-1</sup> band that grows in at pH 13 and 14 at the expense of the 955-cm<sup>-1</sup> band is attributed to the (VO) stretch of the hydroxo adduct, (HO)(VO)TMPyP. The 895/955 cm<sup>-1</sup> intensity ratio at pH 13 and 14 indicates that the pK<sub>a</sub> for ionization of water coordinated to the VO group is ~13.5, only slightly lower than the pK<sub>a</sub> of water itself. Thus binding to (VO)TMPyP produces only a very small enhancement of the acidity of H<sub>2</sub>O, another indication of the low effective charge on the V atom in the VO group. Replacing H<sub>2</sub>O with D<sub>2</sub>O has no discernable effect on either the 955- or the 895-cm<sup>-1</sup> band. Although H-bonding from H<sub>2</sub>O to the VO group is certainly expected, and is seen in the high H<sub>2</sub>O acceptor number and lowered V–O stretching frequency, the change to D-bonding is evidently without influence on the V–O frequency. Table II lists the 6-coordinate V–O frequencies determined in this study, and the shifts relative to the 5-coordinate frequencies in the same solvents.

### Discussion

The V<sup>IV</sup>–O bond can be considered to result from the interaction of V<sup>4+</sup> and O<sup>2-</sup>; an orbital diagram appropriate for a vanadyl porphyrin is given in Figure 10. In addition to the σ-donor interaction between the filled O<sup>2-</sup> p<sub>z</sub> orbital (z is the V–O direction) and the empty V<sup>4+</sup> d<sub>z<sup>2</sup></sub> orbital, there are π-donor interactions between the filled p<sub>x</sub> and p<sub>y</sub> orbitals and the empty d<sub>xz</sub> and d<sub>yz</sub> orbitals. The result is a formal V≡O triple bond, reflected in the high stretching frequency, ~1000 cm<sup>-1</sup>. The bond strength is modulated, however, by molecular interactions at either the V or O atoms and by the electronic properties of the porphyrin ring.

**Solvent Acceptor Effects and Porphyrin Differences.** Because of the polar character of the V–O bond, donor molecules interact at the V end and acceptor molecules at the O end. Both kinds of interactions weaken the V–O bond by counteracting the O →

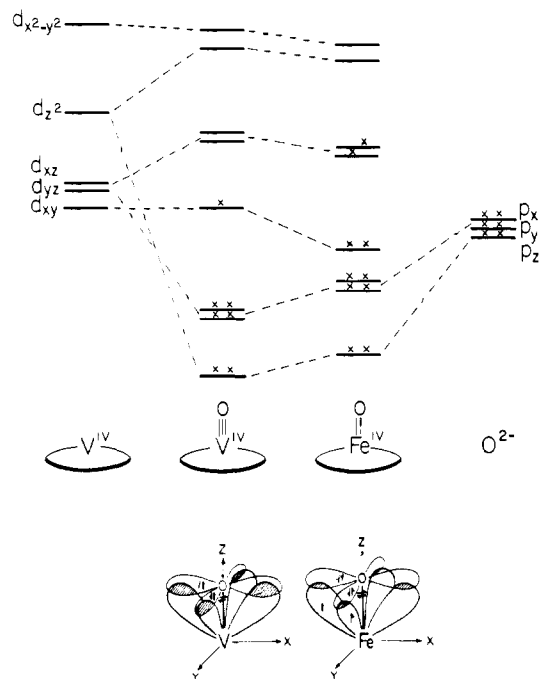


**Figure 10.** Schematic orbital diagram for the V≡O and Fe=O bonds in vanadyl and ferryl porphyrins.

V charge donation in the bond. Thus polar solvents decrease the V–O frequency in proportion to the acceptor strength, as shown in Figures 3 and 4. The acceptor number (AN) is a measure of the electrophilic character of the solvent, developed by Gutman and co-workers from <sup>31</sup>P NMR chemical shifts for the test molecule (C<sub>2</sub>H<sub>5</sub>)<sub>3</sub>PO. The larger the acceptor number the greater the reduction in V–O bond strength, as solvent molecules interact with the electron pairs at the O end of the bond and retard the O → V donation.

The correlation depends in an interesting fashion on the nature of the porphyrin. The influences of porphyrin substituents on axial ligation have been reviewed by Buchler et al.<sup>32</sup> under the category of “cis” effects. The phenyl groups of TPP are found on many criteria to be less electron donating than the ethyl groups of OEP. For example, the redox potential for ring oxidation or reduction is more cathodic for OEP than TPP; the oxidation potential difference of ~0.2 V for (VO)TPP<sup>24</sup> and (VO)OEP (present work) is typical for TPP/OEP analogues.<sup>25</sup> Another example cited by Buchler et al.<sup>32</sup> is that the Ti–O stretching frequency ranges from 955 to 966 cm<sup>-1</sup> for (TiO)OEP but 975 to 980 cm<sup>-1</sup> for (TiO)tetrakis(4-isopropylphenyl)porphyrin. OEP, being more electron donating, is expected to increase the transfer of charge from porphyrin to Ti, and therefore reduce the O → Ti donation. Table I shows, however, that (VO)TPP and (VO)OEP have the same V–O frequency, 1007 cm<sup>-1</sup>, in hexane. Thus with a non-accepting solvent as the reference state, TPP and OEP show the same porphyrin → V donor propensity.

On the other hand, the slopes of the plot of V–O frequency versus solvent acceptor number are significantly steeper for OEP than TPP. Thus OEP does show a stronger donor tendency as the V–O bond polarization by acceptor solvent increases. The donor polarizability of OEP is greater than that of TPP, although they are at the same donor level in hexane. (VO)TMPyP has a significantly higher ν<sub>V–O</sub> when extrapolated to a nonaccepting solvent, 1024 cm<sup>-1</sup>, indicating a weaker donor tendency. This is readily accounted for on the basis of the positive charge of the methylpyridinium substituents. The slope of ν<sub>V–O</sub> versus acceptor number is about the same as for (VO)OEP, however, indicating a significantly greater donor polarizability for methyl pyridinium than for phenyl groups.

(32) Buchler, J. W.; Kokisch, W.; Smith, P. D. *Struct. Bonding* 1978, 34, 80–131.

For (VO)OEP and also (VO)TPP the alcoholic solvents define a line with significantly lower slope than the remaining solvents. We speculate that the associated nature of these solvents inhibits the full expression of their acceptor potential. This is not the case for (VO)TMPyP, however, nor, apparently, for the reference molecule  $(C_2H_5)_3PO$ , upon which the acceptor number scale is based.<sup>31b</sup> Perhaps the H-bond network of the alcohols is broken up in the vicinity of these solutes, because of the tetrapositive charge of (VO)TMPyP, and because of the relatively small polar character of  $(C_2H_5)_3PO$ , compared with (VO)OEP versus (V-O)TPP.

**(VO)OEP<sup>+</sup>  $\pi$ -Cation Radical.** When (VO)OEP is electrochemically oxidized in  $CH_2Cl_2$  the product is an  $a_{2u}$  porphyrin  $\pi$ -cation radical, as revealed by the RR skeletal mode shifts.<sup>29</sup> The effect of the ring oxidation is to shift the V-O frequency up by  $15\text{ cm}^{-1}$ . The direction of the shift is as expected from polarization arguments since the positive charge on the ring reduces the porphyrin  $\rightarrow V$  electron donation and increases the  $O \rightarrow V$  donation. The magnitude of the shift is about as large as seen when comparing (VO)TMPyP with (VO)TPP or (VO)OEP in the limit of a nonaccepting solvent (Figure 4), 1024 versus  $1007\text{ cm}^{-1}$ . (VO)OEP<sup>+</sup> has only one positive charge while VO-(TMPyP) has four, but the latter are located on the peripheral substituents and are farther from the central V atom. Consequently the  $15\text{-cm}^{-1}$  upshift does not seem unreasonable for a purely electrostatic polarization effect.

**Ligand Donor Effects.** In six-coordinate L-V-O species there must be both V-O and V-L stretching modes. The V-L stretching frequency is unknown because the mode is insufficiently enhanced to be detected in the RR spectrum of any of the 6-coordinate species examined. The V-L mode was particularly sought in the RR spectra of the (VO)TMPyP aquo or hydroxo complexes, since its assignment would have readily been confirmed by the expected isotope shifts in  $D_2O$ . No  $D_2O$ -sensitive band was detected, however, in the region below  $700\text{ cm}^{-1}$ .

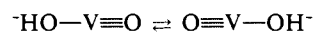
The reason that the V-O mode is strong while the V-L mode is weak is connected with the electronic properties of the resonant excited state, which is porphyrin  $\pi-\pi^*$  in character. The metal-ligand modes are enhanced to the extent that the bond lengths are altered in the excited state.<sup>27</sup> The electronic transition involves population of the lowest unoccupied porphyrin  $\pi^*$  orbitals ( $e_g$ ); these interact with the  $d_{xz}, d_{yz}$  ( $e_g$ ) orbitals on V, which are also involved in the  $O \rightarrow V$   $\pi$ -donor interactions (Figure 9). Consequently the V-O bond is expected to lengthen in the resonant excited state; the high RR intensity of  $\nu_{V-O}$  can be understood on this basis. The L-V coordinate bond, however, does not involve the  $d_{xz}, d_{yz}$  orbitals as directly, and its stretching mode is not significantly coupled to the electronic transition. A similar situation is found in  $Fe^{2+}$  porphyrins with  $\pi$ -acid axial ligands, as in the  $O_2$ <sup>33</sup> and  $CO$ <sup>34</sup> adducts of myoglobin or hemoglobin. The Fe-O and Fe-C stretching bands are enhanced in resonance with the heme  $\pi-\pi^*$  transitions, due to the competition between the  $O_2$  or CO acceptor orbitals and the porphyrin  $\pi^*$  orbitals for the  $Fe^{2+}$   $d_\pi$  electrons. The stretching band of the *trans* imidazole ligand is very weak,<sup>33</sup> however.

In the absence of a change in the V-O force constant the effect of binding a sixth ligand to the vanadyl group would be to raise the V-O frequency slightly due to mechanical coupling with the V-L stretching mode. A model calculation for a triatomic L-V-O oscillator gives  $\nu_{V-O}$  at a frequency  $5\text{--}10\text{ cm}^{-1}$  higher than the five-coordinate value of  $\sim 1000\text{ cm}^{-1}$  when ligands of mass 18 to 65 ( $H_2O$  to imidazole) and V-L force constants of 1 to 2 mdyne/Å (a reasonable range for coordinate bonds) are used. However, an actual weakening of the V-O bond is expected due to electron donation from the sixth ligand, which reduces the  $O \rightarrow V$  donation; L and O compete for the same V acceptor orbitals (*trans* effect<sup>32</sup>). This is the dominant effect for all the adducts investigated, the observed lowerings from the five-coordinate frequencies ranging

from  $8\text{ cm}^{-1}$  for THF to  $75\text{ cm}^{-1}$  for  $OH^-$  (Table II).

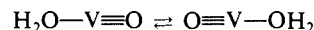
The frequency reduction observed for the hydroxo adduct implies a large reduction in the V-O force constant, partly because the force constant scales with the square of the frequency and partly because for a given force constant the V-O frequency is pushed up by interaction with the V-OH stretching mode. The frequency of the latter is unknown, but for a reasonable range of V-OH stretching force constants,  $1.5\text{--}2.5\text{ mdyne/\AA}$ , model calculations for a HO-V-O system give V-O force constants of  $5.5\text{--}5.6\text{ mdyne/\AA}$ , down by  $\sim 25\%$  from the 5-coordinate value in hexane. The large effect of the *trans*  $OH^-$  ligand, is attributable to the strong  $\pi$ -donor characteristics of  $OH^-$ , which competes significantly with the oxo ligand for occupancy of the  $V^{IV}$   $d_{xz}, d_{yz}$  orbitals. Large  $\nu_{M-O}$  reductions have also been observed when  $CH_3O^-$  is coordinated to  $M^{VO}$  porphyrins,  $M = Mo, W,$  and  $Re$ .<sup>32</sup>

An interesting aspect of the  $895\text{-cm}^{-1}$  V-O stretching band of the hydroxo complex of (VO)TMPyP is its large width,  $32\text{ cm}^{-1}$  (fwhm). The  $955\text{-cm}^{-1}$  band of the aquo complex is also broader,  $23\text{ cm}^{-1}$ , than the V-O band for any of the species studied in the nonaqueous solvents, all of which are  $\sim 12\text{ cm}^{-1}$  wide. Much of the broadening is no doubt due to heterogeneity in the solvent environment associated with the H-bonding properties of water. For the hydroxo complex, however, it is possible that some of the extra width is due to *homogeneous* broadening via rapid interconversion of degenerate tautomers, namely



The rate of the required proton transfer to and from solvent may well approach the vibrational time scale.

This interconversion scrambles the oxo and hydroxo ligands and is undoubtedly the mechanism of the base-catalyzed solvent exchange seen in the  $^{18}O$ -labeling experiments. When (VO)TMPyP is dissolved in  $H_2^{18}O$  at neutral pH, the V-O RR band is shifted to its  $V-^{18}O$  frequency only slowly, over the course of  $\sim 3\text{ h}$ , while at pH 14 the shift occurs within the measurement time. These observations suggest that the exchange reaction for  $(H_2O-V-O)TMPyP$  proceeds via deprotonation of the bound  $H_2O$ , and that the direct interconversion



is very slow, probably because it requires the intermediacy of  $HO-V-OH$ , a high-energy tautomer of  $H_2O-V\equiv O$ .

The ligands Py, ImH, and Im<sup>-</sup> produce  $\nu_{V-O}$  downshifts of  $\sim 21$ ,  $\sim 35$ , and  $\sim 57\text{ cm}^{-1}$ , reflecting increasingly strong donor properties. The basicity of these heterocyclic ligands increases in this order, as does the propensity for  $\pi$ -donation. It is surprising, however, that the shift for ImH is nearly twice as large as for Py, and that the shift for Pip,  $\sim 16\text{ cm}^{-1}$ , is smaller than that for Py, even though Pip is a stronger base. Possibly steric factors are involved because of the tendency of the V atom to be displaced away from the porphyrin plane toward the O atom and the consequent crowding between the ligand and the porphyrin N atoms. The steric demand increases in the order  $ImH < Py < Pip$ . The largest 6-coordinate shift is shown by  $OH^-$ , although it is not as strong a base as Im<sup>-</sup>. The shift augmentation for  $OH^-$  is attributed to its strong  $\pi$ -donor characteristics. The imidazolate ligand is half-way between ImH and  $OH^-$  in its donor strength, as reflected in the  $\nu_{V-O}$  shift. The larger donor strength of Im<sup>-</sup> relative to ImH has previously been demonstrated via the substantial increase, from 211 to  $239\text{ cm}^{-1}$ , in the frequency of the Fe-imidazole stretching band upon deprotonation of the 2-methylimidazole ligand of  $(2-MeImH)Fe^{II}PP$  (PP = protoporphyrin), an analogue of the deoxyheme group in myoglobin, and in reduced peroxidases.<sup>35,36</sup>

Ligation shifts of  $\nu_{V-O}$  are slightly but systematically larger for (VO)TPP than (VO)OEP. This is as expected since the greater donor propensity of (VO)OEP diminishes the  $L \rightarrow V$  donor interaction, but the effect is small. A substantially larger difference is seen when the ImH ligation shift is compared for (VO)OEP

(33) Walters, M. A.; Spiro, T. G. *Biochemistry* **1982**, *21*, 6989-6995.

(34) Tsubaki, M.; Srivastava, R. B.; Yu, N.-T. *Biochemistry* **1982**, *21*, 1132-1140.

(35) Stein, P.; Mitchell, M.; Spiro, T. G. *J. Am. Chem. Soc.* **1980**, *102*, 7795-7797.

(36) Teraoka, J.; Kitagawa, T. *J. Biol. Chem.* **1981**, *256*, 3969-3977.

**Table III.** Trends in  $\nu_{\text{FeO}}$  ( $\text{cm}^{-1}$ ) for Natural and Synthetic Ferryl Porphyrins, and Comparison with  $\nu_{\text{VO}}$  for Analogue Vanadyl Porphyrins

compound	$\nu_{\text{FeO}}$	$\Delta^b$	proposed interaction	analogue	$\nu_{\text{VO}}$	$\Delta^b$
(FeO)TPP; (FeO)OEP <sup>19</sup>	852	0	5-coordinate	(VO)TPP	1007	0
(THF)(FeO)TpivPP <sup>21</sup>	829	23	THF adduct	(THF)(VO)OEP	990	17
(1-MeIm)(FeO)PPDME <sup>22</sup>	820	32	imidazole adduct	(ImH)(VO)OEP	955	52
(1-MeIm)(FeO)TpivPP <sup>21</sup>	807	45	imidazole adduct	(ImH)(VO)TPP	959	48
ferryl Mb <sup>11</sup>	797	55	imidazole weakly H-bonded			
HRP-C II high pH <sup>10,12,13,16,17</sup>	787	65	deprotonated imidazole	(Im <sup>-</sup> )(VO)TPP	936	71
HRP-C II neutral pH <sup>10,12,13,16,17</sup>	775	77	deprotonated imidazole and weak distal H-bond			
CCP-ES	767 <sup>17</sup>	99	deprotonated imidazole and distal arginine H-bond			
	753 <sup>14</sup>					

<sup>a</sup>See discussion. <sup>b</sup> $\Delta$ , frequency lowering relative to the 5-coordinate (MO)TPP. Some portion of  $\Delta$  is attributable to solvent and porphyrin difference, as well as the axial ligand, as discussed in the text.

(33  $\text{cm}^{-1}$ ) and (VO)TMPyP (45  $\text{cm}^{-1}$ ). The same 6-coordinate  $\nu_{\text{V-O}}$ , 960  $\text{cm}^{-1}$ , was observed when (VO)TMPyP was ligated with 1-MeIm, instead of ImH, so that possible effects due to H-bonding of the ImH proton<sup>32,35,36</sup> can be excluded.

**Implications for Ferryl Hemes.** These trends in the V-O stretching frequencies of vanadyl porphyrins are helpful in assessing RR data which is becoming available on the Fe-O stretching frequency of ferryl porphyrins. The Fe-O bond is significantly weaker than the V-O bond due to the  $d^4$ -configuration of  $\text{Fe}^{\text{IV}}$  (see Figure 10). Two of the Fe valence electrons are accommodated in the nonbonding  $d_{xy}$  orbital and the remaining two occupy the  $d_{xz}, d_{yz}$  orbitals, which are involved in the  $\pi$  bonds from the oxo ligand. These two antibonding electrons reduce the formal Fe-O bond order from three to two.

A Fe-O stretching frequency, 852  $\text{cm}^{-1}$ , has recently been reported by Nakamoto and co-workers<sup>19</sup> for (FeO)TPP or (FeO)OEP prepared by laser-induced photolysis of  $(\text{O}_2)\text{FeTPP}$  or  $(\text{O}_2)\text{FeOEP}$  in an  $\text{O}_2$  matrix. The frequency in this nonpolar matrix can be compared with the V-O frequency of (VO)TPP in noncoordinating solvent, 1007  $\text{cm}^{-1}$ . The 155- $\text{cm}^{-1}$  reduction is attributable to the lowered Fe=O bond order. With use of a diatomic oscillator approximation, the Fe-O force constant is calculated to be 5.32  $\text{mdyn}/\text{\AA}$ , 27% lower than the V-O force constant, 7.25  $\text{mdyn}/\text{\AA}$ . This is in good accord with the expected  $1/3$  reduction in the M-O bond order.

The Fe-O bond can be expected to show similar sensitivity to polarization by solvent or ligand interactions as the V-O bond. The actual frequency shift for a given polarization effect will be somewhat diminished, since a given percentage change in the M-O force constant produces a smaller shift when the initial frequency is  $\sim 850 \text{ cm}^{-1}$  rather than  $\sim 1000 \text{ cm}^{-1}$ . Trends in the available data on  $\nu_{\text{FeO}}$  are discussed below in relation to  $\nu_{\text{VO}}$  of reference compounds. Salient comparisons are listed in Table III, in which the close parallelism between  $\nu_{\text{FeO}}$  and  $\nu_{\text{VO}}$  provides support for suggested interactions in the ferryl heme proteins that influence the Fe-O bond strength.

Kitagawa and co-workers<sup>20</sup> report  $\nu_{\text{Fe-O}}$  at 843  $\text{cm}^{-1}$  for (FeO)TMP (TMP = tetramesitylporphyrin) in toluene. The 9- $\text{cm}^{-1}$  reduction from (FeO)TPP is similar to the 6- $\text{cm}^{-1}$  polarization effect of benzene versus hexane (Table I) on  $\nu_{\text{V-O}}$  of (VO)TPP.

Kean et al.<sup>22</sup> have found  $\nu_{\text{Fe-O}}$  at 820  $\text{cm}^{-1}$  for (1-MeIm)-(FeO)PPDME (PPDME = protoporphyrin IX dimethyl ester) in toluene at  $-130^\circ\text{C}$ , 32  $\text{cm}^{-1}$  lower than the (FeO)OEP matrix frequency. The difference coincides with that seen for ImH coordination to (VO)OEP in  $\text{CH}_3\text{CN}$ , but  $\sim 10 \text{ cm}^{-1}$  should be allocated to the polarizing effect of the toluene, so the ligation sensitivity is somewhat smaller for  $\nu_{\text{Fe-O}}$  than  $\nu_{\text{V-O}}$ . On the other hand, Schappacher et al.<sup>21</sup> located  $\nu_{\text{Fe-O}}$  at 807  $\text{cm}^{-1}$  for the "picket fence" porphyrin (1-MeIm)FeO(TpivPP) ((TpivPP) = *meso*-tetrakis( $\alpha$ -pivalamidophenyl)porphyrin). The extra 13  $\text{cm}^{-1}$  lowering relative to (1-MeIm)(FeO)PPDME is attributable partly to the inductive effect of TPP versus OEP-type porphyrins (cf. 4  $\text{cm}^{-1}$  for (ImH)(VO)TPP versus (ImH)(VO)OEP) and partly to the polarizing effect of the pivalamido "pickets", within which the oxo ligand is located. When THF was the ligand, instead of 1-MeIm,  $\nu_{\text{Fe-O}}$  was 829  $\text{cm}^{-1}$ , 22  $\text{cm}^{-1}$  higher. This difference is again somewhat smaller than the 35- $\text{cm}^{-1}$  difference allocable to

THF substitution for ImH in (ImH)(VO)OEP (Table II) when the 10- $\text{cm}^{-1}$  difference due to solvent (THF versus  $\text{CH}_3\text{CN}$ ) is taken into account. Thus, the effects of the trans ligand are parallel, but somewhat smaller, for ferryl than vanadyl porphyrins.

The Fe-O stretch has also been detected by RR spectroscopy for the ferryl group in oxidized heme proteins. The horseradish peroxidase (HRP)-peroxide reaction intermediate compound II, which contains ferryl heme, shows  $\nu_{\text{Fe-O}}$  at 787  $\text{cm}^{-1}$  at pH values above a transition  $\text{p}K_a$  that depends on the isoenzyme, 8.8 for HRP-isoenzyme C (HRP-C) and  $\sim 6.9$  for HRP-isoenzyme A (HRP-A).<sup>10,12,13,16,17</sup> Below this  $\text{p}K_a$   $\nu_{\text{Fe-O}}$  drops to 775  $\text{cm}^{-1}$  for HRP-C (780  $\text{cm}^{-1}$  for HRP-A) and it shifts up slightly, 2-4  $\text{cm}^{-1}$ , in  $\text{D}_2\text{O}$ . These characteristics have been interpreted in terms of H-bonding to the ferryl O atom from a titratable residue, probably the protonated form of a distal histidine. The same residue is no doubt responsible for a perturbed mode of CO binding in the CO adduct of reduced HRP, involving H-bonding to the O atom of the bound CO.<sup>37-39</sup> This H-bond also titrates away at high pH. The  $\sim 10\text{-cm}^{-1}$  reduction of  $\nu_{\text{Fe-O}}$  associated with the neutral pH form is rather small, however, and suggests that the H-bond is fairly weak.<sup>17</sup> Comparison can be made to the 27- $\text{cm}^{-1}$  reduction of  $\nu_{\text{V-O}}$  for (VO)OEP in methanol, an H-bond donor solvent, versus hexane.

For the high-pH form of HRP compound II  $\nu_{\text{Fe-O}}$ , at 787  $\text{cm}^{-1}$ , is 33  $\text{cm}^{-1}$  lower than in the 1-MeIm adduct of (FeO)PPDME. This difference may be due to strong H-bonding from the proximal imidazole N $\epsilon$  atom to a protein acceptor group, or actual deprotonation. In cytochrome *c* peroxidase (CCP) a carboxylate acceptor group from an aspartate residue is known from crystallography to be available for such an H-bond.<sup>40</sup> Bound imidazole H-bond donation has been shown via deoxy heme model compounds<sup>35</sup> to increase the Fe-imidazole bond strength, and for reduced HRP<sup>36</sup> and CCP<sup>18</sup> the Fe-imidazole stretching frequency,  $\sim 245 \text{ cm}^{-1}$ , is much higher than it is in, e.g., Mb (220  $\text{cm}^{-1}$ ),<sup>41</sup> consistent with substantial imidazole character via the H-bond donation. In the  $\text{CN}^-$  complex of native ( $\text{Fe}^{\text{III}}$ )HRP, the proximal imidazole has been shown by NMR<sup>42</sup> to be actually deprotonated, although the proton is retained by the protein, presumably on a nearby carboxylate residue, and reappears on the proximal imidazole when  $\text{CN}^-$  is removed. It is quite likely that formation of the ferryl intermediate is also accompanied by deprotonation. The effect on  $\nu_{\text{V-O}}$  of deprotonating imidazole which is ligated to (VO)OEP or (VO)TPP is to lower it by  $\sim 23 \text{ cm}^{-1}$  (Table II). Thus the 33  $\text{cm}^{-1}$   $\nu_{\text{Fe-O}}$  difference between alkaline HRP compound II and (1-MeIm)(FeO)PPDME is fully consistent with deprotonation.

(37) (a) Evangelista-Kirkup, R.; Smulevich, G.; Spiro, T. G. *Biochemistry* **1986**, *25*, 4420-4425. (b) Smulevich, G.; Evangelista-Kirkup, R.; English, A.; Spiro, T. G. *Biochemistry* **1986**, *25*, 4426-4430.

(38) Barlow, C. H.; Ohlsson, P.-I.; Paul, K.-G. *Biochemistry* **1976**, *15*, 2225-2229.

(39) Smith, M. L.; Ohlsson, P.-I.; Paul, K.-G. *FEBS Lett.* **1983**, *163*, 303-305.

(40) Finzel, B. C.; Poulos, T. L.; Kraut, J. *J. Biol. Chem.* **1984**, *259*, 13027-13036.

(41) Kitagawa, T.; Nagai, K.; Tsubaki, M. *FEBS Lett.* **1979**, *104*, 376-378.

(42) DeRopp, J. S.; Thanabal, V.; LaMar, G. N. *J. Am. Chem. Soc.* **1985**, *107*, 8268-8270.

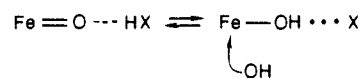
In cytochrome P<sub>450</sub> the axial ligand is thiolate,<sup>43</sup> which is an even stronger donor than imidazolate. Thus the C–O stretching frequency in CO heme adducts, which is a measure of back donation of Fe d<sub>π</sub> electrons in response to the donor properties of the trans ligand, is lower when the trans ligand is thiolate than when it is imidazolate.<sup>44</sup> Consequently, the Fe–O bond is expected to be weakened, and ν<sub>FeO</sub> lowered, even further in the putative ferryl intermediate of the P<sub>450</sub> enzyme reaction than in HRP compound II. We attempted to gauge the effect on ν<sub>V–O</sub> of thiolate coordination to vanadyl porphyrins but were thwarted by decomposition reactions, probably involving thiolate oxidation.

The analogous intermediate for CCP is the ES compound, and its ν<sub>Fe–O</sub> 767<sup>17</sup> or 753<sup>14</sup> cm<sup>-1</sup>, is substantially lower than for HRP compound II. Moreover, it is independent of pH over the range 4–11. Sitter et al.<sup>14</sup> have suggested that the ~35 cm<sup>-1</sup> lowering relative to HRP compound II may be due to a strong H-bond interaction with a distal arginine, which would not be titratable. The crystal structure of the CCP fluoride adduct<sup>45</sup> shows that an arginine residue in the distal region of the native protein swings into place to H-bond with the bound F<sup>-</sup>. A similar interaction seems likely for the oxo ligand of the ES compound. Apparently HRP does not have a similarly accessible arginine. Differences between HRP and CCP with respect to distal interactions have also been observed in the RR signatures of the reduced protein CO adducts.<sup>37</sup>

A ferryl derivative can also be prepared from Mb by treatment with H<sub>2</sub>O<sub>2</sub>. Its Fe–O RR band has been detected,<sup>11</sup> and its frequency, 797 cm<sup>-1</sup>, is 10 cm<sup>-1</sup> higher than that of HRP compound II. As noted above deoxyMb shows a lower Fe–imidazole stretching frequency than reduced HRP, reflecting a weaker proximal histidine H-bond. For Mb the acceptor group for this H-bond is a backbone carbonyl group.<sup>46</sup> The weaker proximal histidine H-bond can readily account for the higher ν<sub>Fe–O</sub>. The Mb frequency is still 23 cm<sup>-1</sup> lower than that of (1-MeIm)-(FeO)PPDME, indicating that the weaker H-bond still has a substantial influence (1-MeIm cannot have an H-bond). In addition, Mb contains a distal histidine residue, which is known to be H-bonded to the outer atom of the O<sub>2</sub> ligand in oxyMb.<sup>47</sup> H-bonding to the ferryl oxo ligand is possible, although the distal histidine would have to move (~1.5 Å) from the vicinity of the outer O<sub>2</sub> atom to that of the monatomic oxo ligand. The Fe–O RR band of ferrylMb is unchanged above pH 6,<sup>11</sup> suggesting that distal H-bonding is absent, or that the distal imidazole pK<sub>a</sub> is appreciably lower than 6.

Kitagawa and co-workers<sup>17</sup> made the interesting observation that the O atom of the ferryl group is rapidly exchanged with H<sub>2</sub><sup>18</sup>O in the neutral pH form of HRP compound II, but not in the high pH form. The mechanisms of this exchange cannot be Fe–O dissociation, in view of the strength of the Fe=O bond, nor is it likely to be trans nucleophilic attack by water. Not only is access to the trans position blocked by the imidazole ligand, but the exchange behavior of (VO)TMPyP suggests that base catalysis is needed even when H<sub>2</sub>O is bound in the trans position (vide supra), whereas the observed exchange in HRP compound II is specific for the neutral pH form. A plausible alternative is cis attack of H<sub>2</sub>O from the distal pocket to form a seven-coordinate intermediate or transition state. This would be augmented by the H-bonding to the ferryl group in the neutral pH form, which would tend to reduce the directionality of the Fe–O bond by reducing the π-bonding. Since the H-bond is relatively weak, the exchange

reaction might be modulated by protein motions that strengthen it. The proposed mechanism can be formulated as



The tautomeric equilibrium lies far to the left, but protein fluctuations can produce transient shifts to the right, during which cis attack may be facile.

### Summary

The V–O stretching RR band of vanadyl porphyrins is strongly enhanced in resonance with the Soret electronic transition, and its frequency is sensitive to molecular interactions that weaken the V≡O triple bond by inhibiting O<sup>2</sup> → V<sup>4+</sup> electron donation:

(1) Solvents lower ν<sub>VO</sub> in proportion to their acceptor number. Alcohols fall on a separate line from other solvents for OEP and TPP, perhaps reflecting their associated character.

(2) Although ν<sub>VO</sub> is the same for (VO)OEP and (VO)TPP in a nonaccepting solvent, the dependence on acceptor number is steeper for (VO)OEP reflecting a larger donor polarizability. (VO)TMPyP likewise has a steeper slope than (VO)TPP but the zero acceptor number intercept is higher; the positively charged methylpyridinium substituents are poorer donors but have higher donor polarizability than the phenyl substituents.

(3) Oxidation of (VO)OEP to the porphyrin π-cation radical increases ν<sub>VO</sub> by 15 cm<sup>-1</sup>. The shift is attributable to the electrostatic effect of ring oxidation.

(4) Binding of a sixth ligand lowers ν<sub>VO</sub> roughly in proportion to the expected ligand donor strength THF < CH<sub>3</sub>OH, H<sub>2</sub>O < Py < ImH < Im<sup>-</sup> < OH<sup>-</sup>. Surprisingly, the frequency shift is smaller for Pip than Py, and only half as large for Py than ImH; steric factors may be superimposed on the donor strengths. The very large OH<sup>-</sup> shift is attributed to the π-donor propensity of OH<sup>-</sup>, which competes directly with the oxo ligand for the V<sup>IV</sup> d<sub>π</sub> vacancies. The degenerate tautomer shift between the OH<sup>-</sup> and O<sup>2-</sup> ligands probably accounts for the pronounced broadening of ν<sub>VO</sub> and the base-catalyzed <sup>18</sup>/<sup>16</sup>O exchange.

These trends illuminate the available data on ν<sub>FeO</sub> in ferryl porphyrins, which is ~150 cm<sup>-1</sup> lower than ν<sub>VO</sub> due to the M–O bond order being reduced from three to two by the extra Fe<sup>IV</sup> electrons. Shifts associated with sixth ligands are somewhat smaller for ν<sub>FeO</sub> and ν<sub>VO</sub>. The ν<sub>FeO</sub> frequencies observed for HRP compound II support the view that the proximal imidazole ligand is protonated or strongly H-bonded to a protein acceptor group, and that the ferryl O atom is weakly H-bonded by a distal residue, probably imidazole. For CCP compound ES an additional interaction, probably strong H-bonding by distal arginine, is required to explain the even lower ν<sub>FeO</sub>.

**Acknowledgment.** This work was supported by DOE grant DE-ACO2-81ER10861. We thank Drs. T. Kitagawa, Y. Nishimura, and J. Terner for communicating results of their work in advance of publication.

**Registry No.** Hn, 110-54-3; Bz, 71-43-2; THF, 109-99-9; Py, 110-86-1; DMF, 68-12-2; Nb, 98-95-3; An, 75-05-8; Nm, 75-52-5; Pip, 110-89-4; (VO)OEP, 27860-55-5; (VO)TPP, 14705-63-6; (VO)TMPyP, 106049-21-2; (H<sub>2</sub>O)(VO)TMPyP, 114490-52-7; (CH<sub>3</sub>OH)(VO)TMPyP, 114490-53-8; (CH<sub>3</sub>OH)(VO)TPP, 114490-54-9; (CH<sub>3</sub>OH)(VO)OEP, 114504-87-9; (C<sub>2</sub>H<sub>5</sub>OH)(VO)TMPyP, 114490-55-0; (Py)(VO)TPP, 114490-56-1; (Py)(VO)OEP, 114490-57-2; (Pip)(VO)TPP, 55866-59-6; (Pip)(VO)OEP, 114490-58-3; (THF)(VO)OEP, 114490-59-4; (ImH)(VO)TMPyP, 114490-60-7; (ImH)(VO)TPP, 114490-61-8; (ImH)(VO)OEP, 114490-62-9; (Im<sup>-</sup>)(VO)TPP, 114490-63-0; (Im<sup>-</sup>)(VO)OEP, 114490-64-1; (OH<sup>-</sup>)(VO)TMPyP, 114504-88-0; (VO)OEP<sup>••</sup>, 62535-02-8; CH<sub>2</sub>Cl<sub>2</sub>, 75-09-2; *i*-PrOH, 67-63-0; EtOH, 64-17-5; MeOH, 67-56-1; ImH, 288-32-4; Im<sup>-</sup>Na<sup>+</sup>, 5587-42-8; D<sub>2</sub>O, 7789-20-0; CHCl<sub>3</sub>, 67-66-3; H<sub>2</sub>O, 7732-18-5; tetrabutylammonium perchlorate, 1923-70-2; 15-crown-5, 33100-27-5.

(43) Champion, P. M.; Stallard, B. R.; Wagner, G. C.; Gunsalus, I. C. *J. Am. Chem. Soc.* **1982**, *104*, 5469–5472.

(44) Gaul, E. M.; Kassner, R. *J. Inorg. Chem.* **1986**, *25*, 3734–3740.

(45) Edwards, S. L.; Poulos, T. L.; Kraut, J. *J. Biol. Chem.* **1984**, *259*, 12984–12988.

(46) Takano, T. *J. Mol. Biol.* **1977**, *110*, 537–568.

(47) Phillips, V. E.; Schoenborn, B. P. *Nature (London)* **1981**, *292*, 81–82.